

Ground state and energy landscape of interlayer Josephson vortex systems

Yoshihiko Nonomura* and Xiao Hu

Computational Materials Science Center, National Institute for Materials Science, Tsukuba, Ibaraki 305-0047, Japan

(Dated: May 25, 2019)

The ground state of interlayer Josephson vortex systems is investigated on the basis of a simplified Lawrence-Doniach model in which spatial dependence of the gauge field and the amplitude of superconducting order parameter is not taken into account. Energy landscape is drawn with respect to the in-plane field, the period of insulating layers including Josephson vortices, and the shift from the aligned vortex lattice. The energy landscape has a multi-valley structure and ground-state configurations correspond to bifurcation points of the valleys. In the high-field region, the shear modulus becomes independent of field and its anisotropy dependence is given by $c_{66} \sim \gamma^{-4}$.

PACS numbers: 74.25.Qt

Introduction. Although interlayer Josephson vortex systems in cuprate high- T_c superconductors have been intensively studied, their phase diagrams have not been established yet even in the ground state. For high in-plane fields, Josephson vortices penetrate into every insulating layer, and the ground state is given by an elongated triangular lattice aligned along the superconducting layers. As the field decreases, such a vortex lattice aligned along the layers becomes unstable owing to the shear instability [1], and the shearing angle of vortex lattices increases continuously [2]. As the field further decreases, the rotated vortex lattices have been considered to be the ground state [3, 4, 5]. The studies mentioned above (except for Ref. [2]) were based on the London model, and effects of the layered structure were included only as geometrical constraint.

This layered structure can be directly taken into account by using the Lawrence-Doniach model. Ichioka calculated [6] the energies of the aligned vortex lattices including vacant insulating layers. Quite recently, Koshelev evaluated [2] the ground-state phase diagram (including the sheared and rotated vortex lattices) based on a simplified Lawrence-Doniach model, in which spatial dependence of the gauge field and the amplitude of superconducting order parameter is neglected. The ground state of this simplified model is completely given by the in-plane field h , the period N between insulating layers including Josephson vortices, and the shift Δ of the vortex lattice from the aligned one. In Ref. [2], Δ is fixed at fractional numbers which correspond to the rigid rotated vortex lattices. In the present study, we draw the full energy landscape for the first time, and find that the energy landscape has a multi-valley structure, and that the ground state for low fields shows systematic deviation from the rigid rotated vortex lattices.

Formulation. When spatial dependence of the gauge field and the amplitude of superconducting order parameter is neglected, the Lawrence-Doniach free energy func-

tional is expressed by the phase component ϕ_n [2] as

$$F\{\phi_n(\mathbf{r})\} = \frac{\phi_0^2}{16\pi^3\lambda_{ab}^2} \int d^3\mathbf{r} \left\{ \frac{1}{2} (\nabla\phi_n)^2 + \frac{1}{(\gamma d)^2} \left[1 - \cos\left(\phi_{n+1} - \phi_n - \frac{2\pi}{\phi_0} dB^x\right) \right] \right\}, \quad (1)$$

where ϕ_0 is the flux quantum, λ_{ab} is the penetration depth in the ab plane, γ is the anisotropy parameter, and d is the inter-layer distance. The distance a between Josephson vortices in the same layer and the period N (see Fig. 1(a)) are related with the in-plane field along the x axis B^x as $\phi_0 = adNB^x$. Since the ground state should be uniform along the field direction, the free energy functional per unit volume is expressed as

$$f\{\phi_n(\bar{y})\} = \frac{\phi_0 B^x}{16\pi^2\gamma\lambda_{ab}^2} u\{\phi_n(\bar{y})\}, \quad (2)$$

$$u\{\phi_n(\bar{y})\} = \frac{1}{\pi} \sum_{n=1}^N \int_0^{\bar{a}} d\bar{y} \left[\frac{1}{2} \left(\frac{d\phi_n}{d\bar{y}} \right)^2 + 1 - \cos(\phi_{n+1} - \phi_n - h\bar{y}) \right], \quad (3)$$

where the following normalized quantities are introduced:

$$\bar{y} \equiv \frac{y}{\gamma d}, \quad \bar{a} \equiv \frac{a}{\gamma d}, \quad h \equiv \frac{2\pi}{\phi_0} \gamma d^2 B^x. \quad (4)$$

By minimizing the free energy functional (3) with respect to ϕ_n , we have

$$\frac{d^2\phi_n}{d\bar{y}^2} + \sin(\phi_{n+1} - \phi_n - h\bar{y}) - \sin(\phi_n - \phi_{n-1} - h\bar{y}) = 0. \quad (5)$$

This differential equation is solved in the unit cell $\bar{a} \times Nd$ (see Fig. 1(a)) with appropriate quasi periodic boundary conditions. In order to search the ground state, the shift from the aligned vortex lattice Δ defined in Fig. 1(a) should also be swept as the in-plane field h .

Another description of the vortex lattice in layered material is shown in Fig. 1(b), where the vector $\bar{\mathbf{a}}$ between the nearest-neighbor vortices in the same layer

*Electronic address: nonomura.yoshihiko@nims.go.jp

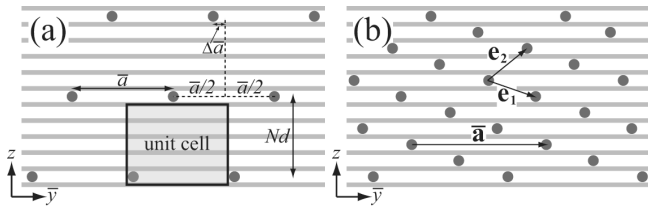


FIG. 1: Definition of (a) the unit cell of a vortex lattice and (b) the labeling of a rigid rotated vortex lattice (here $(n, m, N) = (2, 1, 1)$). Scaled coordinate $\bar{y} \equiv y/(\gamma d)$ is used.

FIG. 2: (a) Energy function $-g$ versus the shift from the aligned lattice Δ and the normalized in-plane field h . Each color stands for the energy function for each N [color online]. The dark solid lines denote the ground state, and the pale solid lines stand for the lowest-energy state (but not the ground state) for each N . The rotated-lattice index (n, m, N) for each ground state configuration is displayed. (b) Top view of the above figure [gif figure appended].

and the unit vectors of the triangular vortex lattice \mathbf{e}_1 and \mathbf{e}_2 are combined with a pair of integers n and m as $\bar{\mathbf{a}} = n\mathbf{e}_1 + m\mathbf{e}_2$. This labeling is based on an equilateral triangular vortex lattice, which we call the “rigid rotated vortex lattice” in the present article. For each (n, m) , there is a corresponding fractional value of Δ . However, it is not trivial that any rigid rotated vortex lattice can be a ground state. As will be revealed below, it is not the case. Hereafter the energy function $g \equiv u + \frac{1}{2} \log h - 1.432$ is used instead of u , following Ref. [2].

Results. The energy landscape of eq. (3) is shown in Fig. 2(a), where $-g$ is taken instead of g because the valley structure is hard to visualize. The ridges in this figure correspond to the valleys in the actual energy landscape. Energy functions for various N ’s are drawn in the same figure, and different colors correspond to different N ’s. The ground state denoted by dark solid lines often jumps between two different values of Δ as drawn in dashed lines. The pale solid lines represent the lowest-energy state (but not the ground state) for each N .

For high h , the aligned $(1, 1, 1)$ vortex lattice corresponds to the ground state with $\Delta = 0$. As the field decreases to $h \approx 1.33$, a sheared lattice with finite Δ becomes the ground state. The shearing angle increases continuously as the field decreases, and such continuous field dependence cannot be represented by the rotated-lattice index. Although the ground state changes to the $(1, 0, 2)$ aligned lattice at $h \approx 0.99$, the sheared vortex lattice state is still the lowest energy state in the $N = 1$ subspace, and it becomes the ground state again at $h \approx 0.80$. The field dependence of Δ is quite small around $h \approx 0.7$, which corresponds to the simplest rigid rotated vortex lattice labeled with $(2, 1, 1)$ and characterized by $\Delta_{\text{rigid}} = 1/7$. Since each ground-state con-

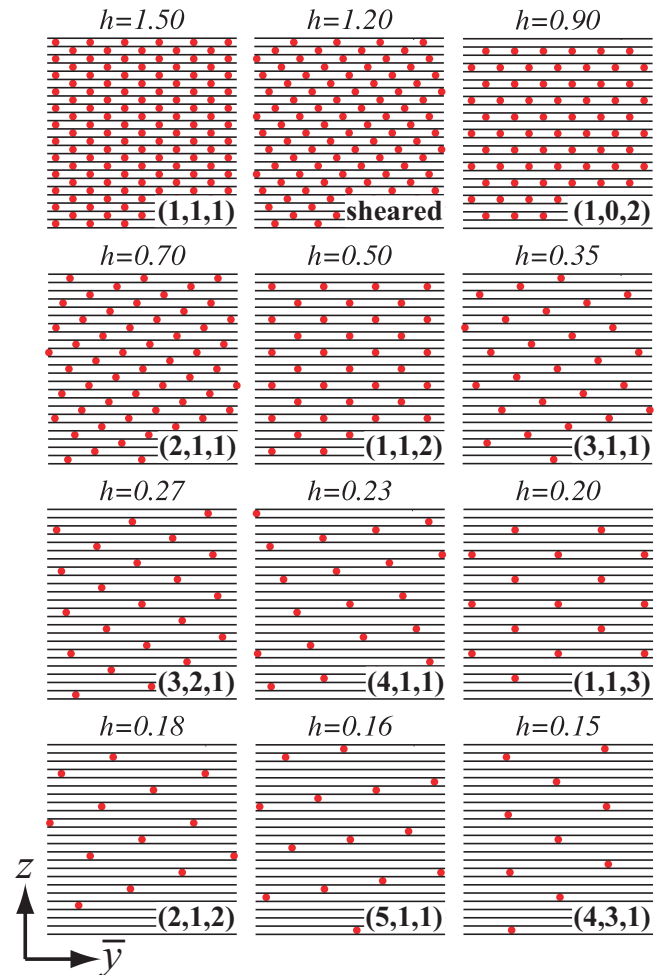


FIG. 3: Ground-state configurations for various in-plane fields h with the corresponding rotated-lattice indices (n, m, N) .

FIG. 4: Energy function $-g$ versus Δ and h in the $N = 1$ subspace, where the dark or pale solid lines are the same as in Fig. 2(a), and the paler solid lines stand for the local energy minima (not the lowest-energy states), and its top view is displayed in the inset. The rotated-lattice indices are given for all the ground-state configurations in this subspace [gif figure appended].

figuration is separated in the energy landscape, these configurations can be labeled by the rotated-lattice indices (n, m, N) , even though the parameter Δ may deviate from the fractional values Δ_{rigid} corresponding to the rigid rotated vortex lattices. Typical ground-state configurations are shown in Fig. 3, where all the rotated-lattice indices (n, m, N) for $h \geq 0.15$ are listed.

Next, the energy landscape in the $N = 1$ subspace is shown in Fig. 4. Here the dark or pale solid lines are defined similarly to the ones in Fig. 2(a), and the paler solid lines denote the local energy minima (not the lowest-

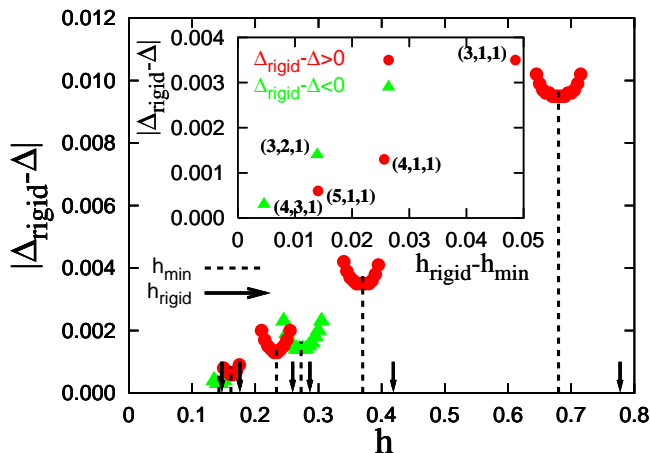


FIG. 5: Deviation of Δ from that of the rigid rotated vortex lattice (Δ_{rigid}) versus normalized field h in the $N = 1$ subspace, and it takes minimum at $h = h_{\text{min}}$ (dashed lines). The normalized fields corresponding to the rigid rotated vortex lattices (h_{rigid}) are marked by arrows. In the inset, the deviation of Δ ($|\Delta_{\text{rigid}} - \Delta|$) at $h = h_{\text{min}}$ is plotted versus that of h ($h_{\text{rigid}} - h_{\text{min}}$) together with the rotated-lattice indices.

energy state in this subspace). Apparently, the rotated-lattice ground states are connected with each other by lines of local energy minima, and the ground states correspond to the bifurcation points of local minima. Such structure of the energy landscape is visualized clearly by the top view shown in the inset, and similar bifurcating structure is expected for $N \geq 2$ at much low fields.

From precise analyses of Δ , we find that the rigid rotated vortex lattices expected from the London model can never be the ground state. The deviation of Δ from the values corresponding to the rigid rotated lattices Δ_{rigid} is plotted versus h in Fig. 5. The inequality $\Delta_{\text{rigid}} - \Delta > 0$ holds for $n \geq m/2$, and vice versa. The field corresponding to the rigid rotated vortex lattice h_{rigid} is marked by arrows in the same figure, and $|\Delta_{\text{rigid}} - \Delta|$ takes minima at $h = h_{\text{min}}$ (dashed lines). The deviation decreases as h decreases, and seems to vanish in the $h \rightarrow 0$ limit. In the inset of this figure, $|\Delta_{\text{rigid}} - \Delta|$ at $h = h_{\text{min}}$ is plotted versus $h_{\text{rigid}} - h_{\text{min}}$.

Finally, we observe the shear modulus c_{66} defined in

$$c_{66} \equiv \frac{d^2 N^2}{a^2} \frac{\partial^2 f}{\partial \Delta^2} \equiv \frac{\phi_0 B^x}{16\pi^2 \gamma \lambda_{ab}^2} \frac{d^2 N^2}{a^2} \tilde{c}_{66}, \quad \tilde{c}_{66} = \frac{\partial^2 u}{\partial \Delta^2}. \quad (6)$$

Field dependence of the scaled shear modulus \tilde{c}_{66} is displayed in Fig. 6. The quantity \tilde{c}_{66} converges to zero in the $h \rightarrow \infty$ limit, and the asymptotic form is evaluated as $\tilde{c}_{66} \approx Ch^{-3}$ with $C \approx 39.4$, which is drawn by the dashed line in Fig. 6. Substituting $\phi_0 = adB^x$ ($N = 1$ for high fields) and eq. (4), we arrive at a field-independent asymptotic form of the shear modulus,

$$c_{66} \approx \frac{\phi_0^2}{(8\pi\lambda_{ab})^2} \frac{C}{2\pi^3 d^2} \gamma^{-4}. \quad (7)$$

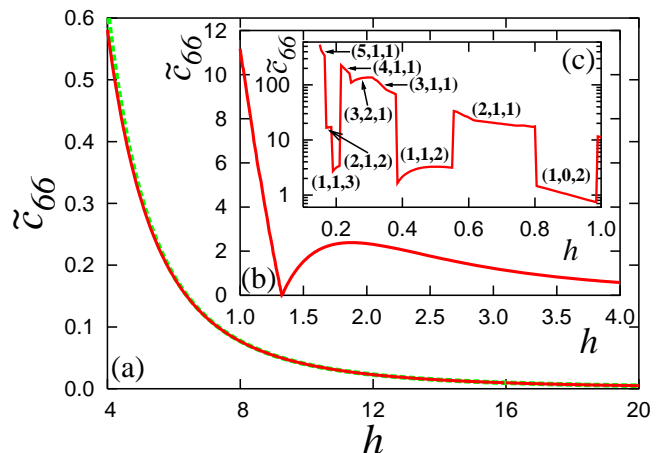


FIG. 6: Field dependence of the scaled shear modulus \tilde{c}_{66} defined in eq. (6). (a) For $h \geq 4$, the dashed line $\tilde{c}_{66} \sim h^{-p}$, $p \approx 2.9993$ is obtained from the least-squares fitting of the data for $16 \leq h \leq 20$. (b) For $1 \leq h \leq 4$, the vanishing point of \tilde{c}_{66} divides the aligned and sheared vortex lattices. (c) For $h \leq 1$, \tilde{c}_{66} is plotted in a logarithmic scale, and the corresponding rotated-lattice indices are displayed.

This is in sharp contrast to the exponentially vanishing c_{66} of the London model [1], and is also different from that of the elastic theory, $c_{66} = [\phi_0 B^x / (8\pi\lambda_{ab})^2] \gamma^{-3}$ [7]. Introducing a “saturated field” $\tilde{B} = C\phi_0 / (2\pi^3 \gamma d^2)$, eq. (7) can be expressed similarly to the elastic theory, and $\tilde{a} \equiv \phi_0 / (d\tilde{B}) = (2\pi^3 / C) \gamma d \approx 1.57 \gamma d$ corresponds to the effective core size of a Josephson vortex.

As the field decreases, \tilde{c}_{66} takes a maximum value around the field for the rigid $(1,1,1)$ vortex lattice ($h = \pi/\sqrt{3}$), vanishes at the shear instability field of the aligned vortex lattice [1], increases again together with the increase of the shearing angle, and jumps when the rotated-lattice index changes. Values of \tilde{c}_{66} are much larger in the $N = 1$ rotated lattices than in the $N \geq 2$ aligned lattices, which suggests that the rotated vortex lattice structure determined by the matching of the lattice and layered structure is much more robust against the shear displacement than the aligned ones.

Discussion. In the London model, only the rigid vortex lattices can be the ground state by definition. Therefore, the sheared vortex lattices are specific to the models including the layered structure explicitly such as the present model. We find that the rotated vortex lattices with Δ_{rigid} cannot be the ground state even at the fields corresponding to the rigid rotated lattices, which is another nontrivial effects of the layered structure.

It would be interesting to investigate how the above description is altered by various kinds of fluctuations. Hu *et al.* [8] studied the phase diagram of interlayer Josephson vortex systems in the vicinity of the melting temperature using the density functional theory. They found the vortex smectic state around the $(n, m, N) =$

(1, 0, 2) state, while no sheared vortex lattice states were observed between the (1, 1, 1) and (1, 0, 2) states. This finding may suggest that the sheared vortex lattice state is affected very much by thermal fluctuations. Study on temperature dependence of the deviation from the rigid rotated lattices would be an interesting future problem.

The screening effect is also studied in the present framework, and we find that the rotated vortex lattices are almost unchanged, while the sheared vortex lattices or the $N \geq 2$ aligned vortex lattices are affected very much. These facts suggest that the rotated vortex lattice structure is robust against the screening effect, similarly to the shear displacement as seen in Fig. 6. Details of this study will be reported elsewhere [9].

Summary. Ground state of interlayer Josephson vortex systems is investigated on the basis of the simplified Lawrence-Doniach model, in which spatial dependence of the gauge field and the amplitude of superconducting order parameter is neglected. The free energy functional is minimized in the unit cell including one Josephson vortex. We draw the energy landscape with respect to the in-plane field, the period of insulating layers including Josephson vortices, and the shift from the aligned lat-

tice.

As the in-plane field decreases, the aligned vortex lattice along superconducting layers changes to the sheared vortex lattice and then to the rotated vortex lattices, in which the shift from the aligned lattice is approximately given by that of the corresponding rigid rotated lattices. Systematic deviation from the rigid configurations is clarified for the first time. The rotated lattices are connected with each other by local minima in the energy landscape to form a multi-valley structure, and the ground states correspond to the bifurcation points of the valleys.

In the high-field region, the shear modulus becomes independent of field and its anisotropy dependence is given by $c_{66} \sim \gamma^{-4}$, quite different from the London theory in which c_{66} decays exponentially with field. This quantity vanishes at the onset of the sheared vortex lattice, and jumps when the rotated-lattice index changes. Large c_{66} for the rotated vortex lattices may signal robustness against fluctuations.

Acknowledgement. We would like to thank Dr. A. E. Koshelev for helpful discussions and sending his article prior to public appearance.

[1] B. I. Ivlev *et al.*, J. Low Temp. Phys. **80**, 187 (1990).
 [2] A. E. Koshelev, cond-mat/0602341.
 [3] L. J. Campbell *et al.*, Phys. Rev. B **38**, 2439 (1988).
 [4] L. S. Levitov, Phys. Rev. Lett. **66**, 224 (1991).
 [5] M. F. Laguna *et al.*, Phys. Rev. B **62**, 6692 (2000).
 [6] M. Ichioka, Phys. Rev. B **51**, 9423 (1995).

[7] V. G. Kogan and L. J. Campbell, Phys. Rev. Lett. **62**, 1552 (1989).
 [8] X. Hu *et al.*, Phys. Rev. B **72**, 174503 (2005).
 [9] Y. Nonomura and X. Hu, in preparation.

This figure "fig2.gif" is available in "gif" format from:

<http://arxiv.org/ps/cond-mat/0603282v1>

This figure "fig4.gif" is available in "gif" format from:

<http://arxiv.org/ps/cond-mat/0603282v1>